Enhancement of human bladder carcinoma cell chemosensitivity to Mitomycin C through quasi-monochromatic blue light (λ=453 nm)

Lisa Hegmann
Department for Orthopedics and Trauma Surgery, Medical Faculty and University Hospital Düsseldorf, Heinrich-Heine-University Düsseldorf

Sofia Sturm
Department for Orthopedics and Trauma Surgery, Medical Faculty and University Hospital Düsseldorf, Heinrich-Heine-University Düsseldorf

Günter Niegisch
Department of Urology, Medical Faculty and University Hospital Düsseldorf, Heinrich-Heine-University Düsseldorf

Joachim Windolf
Department for Orthopedics and Trauma Surgery, Medical Faculty and University Hospital Düsseldorf, Heinrich-Heine-University Düsseldorf

Christoph V. Suschek (suschek@uni-duesseldorf.de)
Department for Orthopedics and Trauma Surgery, Medical Faculty and University Hospital Düsseldorf, Heinrich-Heine-University Düsseldorf

Article

Keywords: bladder tumor, urothelial cancer, chemotherapy, Mitomycin C, blue light, reactive oxygen species, cell death

Posted Date: July 29th, 2022

DOI: https://doi.org/10.21203/rs.3.rs-1869826/v1

Abstract

Human urothelial bladder carcinoma (uBC) is the second most tumor entity of the urogenital tract. As far as possible, therapy for non-muscle invasive uBC takes place as resection of the tumor tissue, followed by intravesical chemotherapy or immunotherapy. Because of the high recurrence rate of uBC, there is a need for improved efficiency in the treatment. In the present *in vitro* study we have evaluated a new approach to enhance the cytotoxic efficiency of Mitomycin C (MMC), which is commonly used for intravesical treatment of uBC on the relevant urothelial cancer cell line RT112. For that we used quasi-monochromatic blue light (453±10 nm) at non-toxic dose of 110 J/cm^2 as an additive stimulus to enhance the therapeutic efficiency of MMC (10 µg/ml). We found, that blue light exposure of RT112 cells led to a very strong increase in intracellular production of reactive oxygen species (ROS) and to a significant reduction of all function parameters of mitochondrial respiration, including basal activity and ATP production. Although not being toxic when used as a single impact, together with MMC blue light strongly enhanced the therapeutic efficiency of MMC in the form of significantly enhanced cytotoxicity via apoptosis and secondary necrosis. Our results clearly show that blue light, most likely due to its ability to increase intracellular ROS production and reduce mitochondrial respiration, increased the cytotoxic efficiency of MMC and therefore might represent an effective, low-side-effect, and success-enhancing therapy option in the local treatment of bladder cancer.

Introduction

Urothelial bladder carcinoma (uBC) is the second most tumor entity of the genitourinary system. New cases in the year 2020 amount to more than 573.000 with a number of deaths of more than 210.000 patients worldwide. About 75% of newly diagnosed urothelial bladder carcinoma belong to the group of non-muscle-invasive tumors (Ta, T1, Cis) [1,2]. Of these, 20–25% progress to muscle-invasive disease during patients' lifetime [3]. Whereas muscle-invasive tumors normally have to be treated by radical cystectomy, therapy of non-muscle-invasive tumors is focused on retaining the bladder. According to the guidelines [1], first line therapy of locally limited tumor is resection of the tumor tissue as a transurethral removal of bladder tumor (TURBT). Although the tumor tissue can be eradicated by this, the recurrence rate is relatively high. About 31% – 78% of the patients will develop a recurrence or new occurrence of urothelial carcinoma within 5 years [4].

In order to delay progression of the tumor or reduce recurrence, resection is mostly followed either by chemotherapy as an intravesical infusion within 24 hours post TURBT (so-called early instillation therapy). Most commonly, Mitomycin C (MMC) is used in this setting [5]. Combining these two treatments could significantly decrease the recurrence risk by 35% but nevertheless a significant part of patients, especially intermediate- and high-risk patients according to the EORTC classification will develop a relapse within 5 years [6]. Therefore, additional therapeutic approaches to reduce the rate of recurrence for these patients are either intravesical *Bacillus Calmette-Guérin* (BCG) or chemotherapeutic instillations post TURBT applied as several repetitions over a longer period of time [1,7–9]. Again, MMC is one of the

chemotherapeutics most commonly applied in this setting. While notable side effects of the BCG instillation, for example cystitis in up to 90% of the patients, as well as fever, granulomatous inflammation of the prostate gland, pneumonitis, bladder contracture or even anaphylaxis have been described, MMC instillations are generally well tolerated [10,11]. However, retrospective analysis suggest that while both MMC and BCG significantly decrease recurrence rate, MMC seem to be inferior with regard to the prevention of tumor progression towards muscle invasion [12].

As a result, there is a clear desire to improve adjuvant therapy of non-muscle invasive uBC. This can be achieved by increasing the specificity or by increasing the effectiveness of the chemotherapy. As a result, lower doses of the chemotherapeutic agent could be used to achieve the desired therapeutic effect, which would both reduce treatment costsas well as therapeutic burdenof the patient. However, even more important, this may retard tumor growth and reduce both the rate of cancer recurrence and progression.

A very simple but extremely effective adjuvant therapy would be the combination of a chemotherapeutic agent and phototherapy. Phototherapy on its own is already an established and widely used form of therapy [13]. Either the direct therapeutic effect of light is used, or the light effect is only achieved through the use of photosensitizers or is further intensified by them [13,14]. For example, doxorubicin was shown acting as a photosensitizer, if activated by blue light irradiation (450 nm), and leads to an increase in oxidative damage in the form of enhanced intracellular generation of reactive oxygen species (ROS) which in turn leads to increased cytotoxicity and decreased cell viability in the treated area [15]. Another example is the combined use of acridine orange, an DNA intercalating dye which can be activated by blue light at approximately 450 nm. As single stimuli both of them do nearly have no effect on the human bladder carcinoma cells, but combined, the treatment is able to significantly reduce tumor cell viability and enhance the activity of caspase-3 and caspase-7 [16]. In general, blue light of the above-mentioned wavelength of approximately 450 nm is a very interesting medium for modulating cell viability, whether used alone or in combination with other therapeutic approaches. Although blue light, in contrast to UVA light, is not toxic or cell-damaging even in very high doses of up to 400 J/cm^2, it can inhibit the proliferation, migration and differentiation of fibroblasts and keratinocytes from 80 J/cm^2 [17–19]. Additionally, an inhibition of cell proliferation, migration and a reduction of cell viability could be shown in melanoma, colon carcinoma and promyelocytic leukemia cells, if irradiated with blue light LED [20–22]. Furthermore, it could be observed that blue light exposure leads to a collapse of mitochondrial membrane potential due to increased ROS generation suggesting the induction of mitochondrial damage [23–25]. In general, it seems to be the case that blue light via the interaction with flavin residues of flavin-containing enzymes not only initiates the production of ROS, which in principle is damaging, but also substantially reduces or inhibits the energy metabolism of the cell through the interaction with corresponding enzyme systems [26].

In particular these properties of blue light that represent a very promising aspect of its therapeutic efficacy, especially when combined with another potent therapeutic agent. The study presented here

evaluates whether and to what extent blue light has an additive or synergistic effect on the cytotoxic behavior of Mitomycin C towards urothelial bladder cell carcinoma cells.

Materials And Methods

Materials

If not otherwise indicated, all chemicals, antibodies, and assay kits were purchased from Sigma-Aldrich Chemie GmbH (Munich, Germany). The human bladder carcinoma cell line RT112 was kindly made available by Dr. J. Fogh (New York, NY), Dr. M. A. Knowles (Leeds, UK) and Dr. B. Grossman (Houston, USA).

Cell lines and cell culture

In our experiments we used the urothelial cancer cell line RT112 showing an epithelial-like morphology.[27] The RT112 cell line was cultivated in the form of adherent monolayer in RPMI 1640 Medium containing 1 g glucose/L (Life Technologies Ltd.; Paisley, UK), supplemented with 5% heat inactivated fetal bovine serum (Fetal Bovine Serum Gold, PAA Laboratories GmbH; Cölbe, Germany), 1% Penicillin/Streptomycin (PAN-Biotech GmbH; Aidenbach, Germany) and 1% sodium pyruvate (Life Technologies Ltd.; Paisley, UK) in T175 culture flasks (CELLSTAR® Cell Culture Flasks 175 cm^2 red filter cap, Greiner Bio-One GmbH; Kremsmünster Austria). Reaching a confluence of 70–80% of confluence, cells were sub-cultured. In order to detach cells, cultures were incubating with 1% trypsin/EDTA solution (PAN-Biotech; Aidenbach, Germany) for 5 min at 37°C. Trypsin activity was neutralized by using a trypsin neutralizer (Life Technologies Ltd.; Paisley, United Kingdom). Cell cultures were maintained in a humidified incubator (95% air and 5% CO_2 at 37°C).

Blue light emitting source

As blue light emitting source we used a 12 x 10 cm LED-arrays with 60 LEDs emitting quasi-monochromatic light with a maximum intensity at 453 ± 10 nm (royal blue). The light sources used here were designed by Philips Research (Aachen, Germany) and the irradiance of the LED arrays was characterized using an Ulbricht sphere. Cell cultures in the current study were irradiated with an irradiance of 39 mW / cm2 at a distance of 5 cm. Routinely, we tested the heat development during the irradiation of 2 ml PBS in a 6-Well cell culture plate (Greiner Bio-One GmbH; Kremsmünster, Austria) corresponding to our experimental setup. We observed an increase in temperature of 1–2°C during the 10 minutes light exposure but sample temperature never exceeded 33°C. The degree of evaporation we determined as the result of the irradiation was so low that the possible osmotic effects of the light-exposed sample were negligible. In order to achieve comparable conditions, cell culture plates containing the control samples were located in a windowed heating cabinet at 33°C.

Chemotherapy

Mitomycin C (MMC; medac GmbH; Wedel, Germany), an alkylating chemotherapy which binds covalently to the DNA, leads to cross-linking and therefor inhibits the replication of the DNA [28] was obtained from the local university pharmacy at a concentration of 1 mg/ml. Due to data of preliminary works [29–31] and our own experiments we used MMC in a concentration of 10 µg/ml for all further experiments.

Experimental setup

For experiments, cells were transferred to transparent multi-well culture plates and were cultivated in culture medium overnight at 37°C and 5% CO_2 to achieve adherence and a nearly confluent layer. Prior irradiation with blue light (110 J/cm^2 with 453 nm) culture medium was replaced by PBS (2 ml /well of the 6-well plates, 1 ml for 12-well plates, 0.5 ml for 24-well plates, 200 µl for 96-well plates). After light exposure, PBS was replaced by culture medium without or containing 10 µg/ml Mitomycin C. At time points indicated cells or cell samples were collected for the different analyses.

MTT Assay

At time points indicated cells were incubated in the dark with 100 µl MTT solution (Thiazolyl Blue Tetrazolium Bromide) reaching a final concentration of 0.5 mg/ml for 2 hours at 37°C. After aspiring the solution, 200 µl of DMSO was added and again incubated for 10 minutes. Afterwards 100 µl of this solution was transferred to a microtiter plate and absorbance was measured by a multilabel counter (Multilabel Counter VICTOR™ V Multilabel counter, Perkin Elmer; Waltham, United States) at a wavelength of 590 nm.

Detection of apoptosis

Apoptotic events in the treated cell cultures in the form of relative amount of hypodiploid nuclei were quantified by FACS analysis (Flow cytometer FACS Calibur, BD Bioscience; Heidelberg, Germany) by the method described by Riccardi and Nicoletti [32]. As positive control we used the effective apoptosis-inducing agent Staurosporin at a concentration of 1 µg/ml.

Immunofluorescence-based quantification of living, apoptotic, and necrotic cell death

In order to differentiate and quantify living, apoptotic, and necrotic cell death we used three analytic fluorescence dyes. Respective cell cultures were incubated for five minutes with fluorescein diacetate (FDA, 2 µg/ml; Santa Cruz Biotechnology; Texas, United States), Hoechst 33342 dye (0.5 µg/ml), and/or propidium iodide (PJ, 0.5 µg/ml). The non-fluorescent FDA enters into viable cells and after cleavage by active esterases FDA can be detected as a green fluorescent coloring of living cells, as [33], H33342 stains the chromatin of living cells by blue fluorescence and thus allows to evaluate nuclear morphology of apoptotic cells, whereas PJ only penetrates “leaky” membranes and thus is an excellent indicator for necrotic cells which glow in red fluorescence [33].

Cellular ATP content

To explore the path of cell death due to the chemotherapy, influenced by the irradiation of blue light more detailed, we investigated the ATP level in the cells after treatment. In this case we used the ATP Assay (ATP Kit #LBR-T010, Biaffin GmbH&Co KG; Kassel, Germany) according to the manufacturer's specifications.

Detection of intracellular generation of reactive oxygen species

Cells were seeded in a density of 5 x 10^5 cells/cm^2. After 24 h medium was removed and cells were washed three times with PBS. Then cells were incubated with 50 µM DCFDA solution in PBS at 37°C and 5% CO_2 for 1 h. DCFDA-solution was removed and cells were washed three times with PBS. Fluorescence was measured in a plate reader (Perkin Elmer VICTOR3™ V Multilabel Counter Model 1420, Waltham, Massachusetts) at an excitation of 495 nm and an emission of 529 nm.

Western Blot

Western Blot analysis of the respective protein expression patterns was perform exactly as described previously [34]. As primary antibodies we used antibodies for PARP (Rabbit anti PARP polyclonal antibody #9542; Cell Signaling Technology®; Leiden, Netherlands), Nrf2 (Rabbit anti Nrf2 monoclonal antibody #12721; Cell Signaling Technology®; Leiden, Netherlands), BAX (Santa Cruz Biotechnology; Texas, United States) and yH2AX (Santa Cruz Biotechnology; Texas, United States) and their corresponding second antibodies (Goat Anti-Mouse Immunoglobulin #P0447; Agilent Technologies; Santa Clara, United States; Goat Anti-Rabbit Immunoglobulin #D0487; Agilent Technologies; Santa Clara, United States). In order to normalize the results, the gel was visualized (ChemiDoc™MP Imaging System; Bio-Rad Laboratories GmbH; München, Germany) before and after the blotting process. The results were calculated as relatively intensities by the help of the software ImageLab™6.0 (Bio-Rad Laboratories GmbH; München, Germany).

Cell preparation for Seahorse assay

In order to detect mitochondrial respiration oxygen consumption rates (OCR), were used the Agilent Seahorse XF24 extracellular flux analyzer (Seahorse Bioscience, North Billerica, MA) exactly as described [35]. Cells were seeded in the respected cell culture plates at a density of 3 x 10^4 cells/well in 200 µl DMEM medium containing 10% FCS and cultures were maintained overnight in 37°C incubator with 5% CO_2. In addition to a sham treated culture plate, in a second plate cells were irradiated in PBS buffer with blue light (453 nm) with dose of 110 J/cm^2. After irradiation PBS was discarded and cells were maintained in DMEM growth medium. One hour after light exposure in each well 150 µl of the medium was removed. After washing the plate two times 500 µl prewarmed XF base medium containing glucose (25 mM), glutamine (2 mM), and sodium pyruvate (1 mM) was added in each well making the final volume of 550 µl. The 96-well cartridge containing the cells was then automatically calibrated by the Seahorse XF24 analyzer. The following Mito Stress Test Assay was performed according to the protocol described by

Butler et al. [36]. OCRs were detected under basal conditions followed by the sequential addition of oligomycin A (0.25 µM), an effective ATP synthase inhibitor, carbonyl cyanide-*p*-trifluoromethoxyphenylhydrazone (FCCP, 10 µM), a potent mitochondrial oxidative phosphorylation uncoupler, and rotenone/antimycin A (10 µM each), rotenone, a complex I inhibitor, and antimycin A, a complex III inhibitor. Thus we were able to estimate the contribution of blue light exposure for basal respiration, proton leak, maximal respiration capacity, spare reserve respiration capacity, nonmitochondrial respiration, and ATP-linked respiration of the irradiated tumor cells.

Additionally, in order to evaluate the impact of blue light exposure on the capacity of the glycolytic pathway after glucose starvation we used the Agilent Seahorse Glycolysis Stress Test. The assay was performed according to the manufacturer's recommendations and protocols. The evaluation of the extracellular acidification rate (ECAR) as an indicator of glycolysis is a common strategy to address the conditions of this energy-producing metabolic pathway [5]. Cells are driven towards glycolysis and their ability to increase glycolytic activity is assessed in order to meet metabolic and bioenergetic requirements. Non-glycolytic acidification is assessed through glucose starvation. The assay measures basal glycolysis after addition of 10 mM D-glucose, glycolysis capacity upon blockage of mitochondrial ATP production using 0.25 µM oligomycin, and glycolytic reserve after addition of 2-Desoxy-D-glucose (100 mM).

Statistical analysis

All values were reported as means ± SD and derive from the indicated number of independent experiments. The statistical analysis was done with GraphPad Prism 8.0. Data were analyzed using an unpaired t-test with $p < 0.05$ considered as to be significant.

Results

Impact of blue light (453 nm) on Mitomycin C induced cell death of RT112 cells

When using the MTT viability assay we found that compared to untreated RT112 control cultures, irradiating the cells alone with blue light (110 J/cm^2) or incubating the cells with Mitomycin C (10 µg/ml) each led to a clearly recognizable but not statistically significant decrease in the number of vital cells (Fig. 1A). However, a combined treatment of the RT112 cell cultures with blue light plus Mitomycin C led to a significantly increased toxicity compared to the treatments with blue light or Mitomycin C alone (Fig. 1A).

In addition to the MTT assay already mentioned, we also quantified the extent of the increase in cell toxicity induced by blue light with the help of fluorescence-based analysis of toxic events in general and, using FACS technology, the apoptotic cell death in particular. Using the fluorescent dyes used here, we were able to distinguish living cells from apoptotic and necrotic cells (Fig. 1C), to differentiate between

necrotic and apoptotic cell nuclei (Fig. 1D) and to recognize different stages of apoptotic nuclei (Fig. 1E). In the quantitative evaluation of the necrotic cells marked by the propidium iodide, we were able to confirm the findings obtained with the help of the MTT assay. In RT112 cultures that were treated with blue light plus Mitomycin C, we were able to achieve a significantly higher proportion of necrotic cells than after treatment with the individual measures (Fig. 1B).

However, the increased cytotoxicity of Mitomycin C that we were able to achieve through the blue light was not only based on necrotic cell death, but also on apoptosis. In the RT112 cultures treated with Mitomycin C plus blue light, we were able to detect a strong and significant increase in the number of hypodiploid, apoptotic nuclei when compared with the frequency of corresponding apoptotic events in RT112 cultures treated with Mitomycin C or blue light alone (Fig. 2).

We also considered the influence of the additive treatment of tumor cells with Mitomycin C plus blue light on the expression of the proapoptotic protein Bax and cPARP, an important parameter for the activity of effector caspase-3, as key molecular parameters of apoptotic cell death. As we show in Fig. 3, blue light also produced a significant apoptosis-enhancing effect at the level of these two parameters. Thus, the light exposure of RT112 cultures treated with Mitomycin C led to an increased Bax protein expression as compared to the control cultures and cultures treated with Mitomycin C alone (Fig. 3A). With regard to the influence on PARP metabolism, we were able to determine that blue light had no influence on the level of PARP protein expression either alone or in combination with Mitomycin S (Fig. 3B). But the combined treatment of the RT112 cultures with blue light plus Mitomycin C induced a sharp increase in the production of cPARP, the active caspase-3 cleave product of PARP. This increase was statistically significantly higher than the sPARP generation in the control cultures and in RT112 cell cultures treated with blue light or Mitomycin C alone (Fig. 3B).

Blue light significantly modulates molecular key parameters of energy metabolism and ROS production in RT112 cells

In the search for further molecular mechanisms of the above-described effect of blue light on the RT112 tumor cells, we observed that blue light used alone or in combination with Mitomycin C significantly reduced ATP production, as compared to respective ATP values in control tumor cell cultures or Mitomycin C treated RT112 cultures (Fig. 4A). In parallel, we observed that exposure of RT112 tumor cells to blue light led to a strong and statistically significant increase in intracellular ROS production of more than eight-fold (Fig. 4B).

The modulative influence of blue light on the two last-mentioned parameters prompted us to evaluate whether and what influence blue light has on mitochondrial respiration and glycolysis of the light-exposed RT112 tumor cells. The results show that one hour after exposure to light, the respiratory chain was almost completely inoperative and no longer responded to the effects of the various function inhibitors (oligomycin, rotenone, antimycin A) and activators (FCCP) used (Fig. 5A). With regard to the individual mitochondrial function parameters, we observed a strong significant decrease in basal activity,

ATP production, maximum respiration, spare respiration capacity, non-mitochondrial oxygen consumption and coupling efficiency after irradiation (Fig. 5B-5G).

We also observed similar results in the context of the evaluation of the effect of blue light on the glycolysis of the irradiated cells (Fig. 6A). Here we were able to observe a significantly reduced glycolysis rate in light-exposed RT112 tumor cell cultures after the addition of glucose, as well as a significantly lower maximum glycolytic capacity and glycolytic reserve (Fig. 6B-6E).

Discussion

For thousands of years, humans have been using the light emitted by the sun as a therapeutic agent against various skin diseases [37,38]. The therapeutic potential of light, in particular light, which alone or in combination with appropriate photosensitizers generates reactive intermediates with therapeutic potential, also including reactive oxygen species (ROS), is of steadily increasing interest in modern medicine [39]. In contrast to high-energy types of radiation such as ultraviolet radiation, blue light with a wavelength of 453 nm is not able to directly generate ROS by splitting molecules or applying energy to oxygen molecules due to its relatively low energy content. Nevertheless, the intracellular generation of reactive oxygen species (ROS) appears to be the relevant molecular mechanism for the effects of exposure to blue light [40–42].

Contrary to what is often assumed, the production of reactive oxygen species ensured by cells own enzyme systems represents a normal cell-physiological process for the control or induction of different physiological signaling pathways. Thus, ROS play an important role in immunity, cell growth and cell signaling. However, in excess, ROS are deadly to cells and the overproduction of these molecules leads to a wide variety of serious diseases [43,44]. The enzymes involved in ROS production are e.g. flavoenzymes of the mitochondrial respiratory chain, in particular NADH dehydrogenase (complex I) and isoenzymes from the NADPH oxidase family (NOX) but also other like 5-lipoxygenase or xanthine oxidoreductase (XOR) [45]. In the functioning of flavoenzymes, the natural substrates NADH or NADPH play the role of reduction equivalents and serve as electron donors for the reduction of the flavin residues. Only the reduced form guarantees a targeted and controlled transfer of electrons to an oxygen molecule and thus the generation of superoxide radical anions (O_2^-.) and H_2O_2 [46,47]. In contrast to the physiological function of the flavoenzymes, the interaction with blue light leads to a photoreduction of the flavin content of the enzyme due to the absorption properties of flavin residues without participating in the natural substrate NADH or NADPH [48]. Immediately after the light-induced flavin reduction, a process of flavin reoxidation begins. This process takes place in a light-independent reaction and, as under physiological conditions, leads to electron transport to oxygen molecules and thus also to the formation of ROS in the form of superoxide radical anions or hydrogen peroxide [46]. However, since the enzyme has no activity control via a feedback mechanism, e.g. the regulation of substrate consumption, the level of ROS production by the flavoenzyme is solely a function of the light dose. Depending on the light dose, very high amounts of ROS

can be generated. So, it is not surprising that we were able to observe such a strong ROS-inducing effect of blue light also in the RT112 bladder cancer cell line used here.

The biological responses observed as a result of blue light increased ROS production include a reduction in migration, proliferation and differentiation of the various cell types exposed to blue light, and above a critical threshold of ROS production it can negatively affect cell viability and become cytotoxic [18,40,48,49]. In order to be able to better record additive or synergistic effects of blue light with the chemotherapeutic agent, we were very careful in the study presented here to use a light dose that, when applied alone, could not induce any significant cytotoxicity. It should of course not go unmentioned that blue light can also have a strong cytotoxic effect, depending on the dose used and the frequency of radiation. For example, Zhang et all were able to show that long irradiation of HL-60 myelogenous leukemia cells with blue light (456 nm) alone led to strong cytotoxicity in the light-exposed cell cultures. The predominant mode of induced cell death was apoptosis, accompanied by all the typical features of caspase-3 controlled apoptosis [21].

Nevertheless, using the chosen non-toxic light dose we observed a significant increase in Mitomycin C toxicity in RT112 bladder cancer cell cultures exposed to blue light. We could not clearly determine the type of increased cell death. We originally assumed that the combined use of the chemotherapeutic agent plus blue light would increase cell death via apoptosis. We were able to partially confirm this expectation. We observed a significant increase in apoptosis, accompanied by a significant increase in the expression of the pro-apoptotic protein Bax and a significantly increased rate of the caspase-dependent degradation of PARP. Overall, this scenario indicates a significantly increased rate of caspase-3 mediated apoptosis. We attribute this increased rate of apoptosis to the greatly increased intracellular production of ROS, which are known to be very effective inducers of apoptosis [50,51].

On the other hand, we also observed a strong and significant increase in secondary necrosis. Apoptotic cell death is a finely tuned and programmed cell death which requires energy to be carried out successfully. If a cell carrying out the apoptotic program no longer has the required energy sources in the form of ATP, it stops this cell death program at the corresponding point in the mechanism and becomes necrotic (secondary necrosis) [52]. This is primarily the case when a damaged cell no longer has sufficient glycolytic or mitochondrial ATP synthesis or is unable to form ATP due to a lack of substrates. This finding of the increased rate of secondary necrosis prompted us to characterize the influence of blue light on the energy metabolism of the RT112 cancer cells used here. In fact, using SeaHorse technology, we were able to find that irradiation of the RT112 cultures with blue light induced a complete breakdown of the mitochondrial respiratory chain and a significant reduction in ATP synthesis. We consider this blue light-induced breakdown of the mitochondrial respiratory chain to be the causal mechanism for the increased rate of secondary necrosis in irradiated RT112 cultures. Of course, the question arises as to why the irradiation of the cells as a single stimulus led to a greatly increased ROS production and mitochondrial breakdown, but did not lead to increased toxicity of the cells. As we were recently able to show with human skin fibroblasts, the decoupling of the respiratory chain shown here is a reversible process after exposure to blue light. Depending on the light dose used, the mitochondrial respiratory

chain recovers quite quickly and showed its original activity potential after just 18 to 24 hours. This temporal course therefore makes sense that in the context of a combination therapy, the addition of the chemotherapeutic agent, as carried out by us, takes place shortly after the radiation, at the time of the greatest ROS exposure and ATP production inhibition.

As a pure in vitro study, the results of our study here are of course only of limited significance with regard to therapeutic clinical use. Nonetheless, our data show that using modern endoscopy techniques, combined simultaneous or sequential local application of a chemotherapeutic agent and blue light can represent an effective treatment option for certain types of bladder cancer. Such a therapy option could be individually adapted to the respective patient by using higher doses of light and further promote the success of the therapy. By using special templates that sharply delimit the area to be treated, one could also protect healthy areas in the treatment area from possible side effects of the therapy.

Declarations

Authors' contributions

Lisa Hegmann: conception, collection and assembly of data, study design, data analysis and interpretation, manuscript writing

Sofia Sturm conception and study design, collection and assembly of data

Günter Niegisch: data analysis and interpretation

Joachim Windolf: final approval of manuscript, data analysis and interpretation,

Christoph V. Suschek: conception and study design, data analysis and interpretation, manuscript writing

Ethics approval and consent to participate

In the context of the project only commercially available cell lines were used, no samples from patients or voluntary donors were used, so that no special ethical-relevant aspects have to be observed and corresponding explanations have to be made.

Consent for publication

The present manuscript does not contain any kind of individual person’s data in any form.

Availability of data and material

The datasets used and/or analyzed during the current study are available from the corresponding author on reasonable request.

Funding

This work was supported by the Medical Faculty of the Heinrich Heine University Düsseldorf and by a grant from the Düsseldorf School of Oncology to L.H.

Acknowledgements

We thank Sabine Lensing-Hoehn, Christa Maria Wilkens, Samira Seghrouchni, and Jutta Schneider for technical assistance.

Disclosure Statement

The authors whose names are listed above certify that they neither actually nor potentially have any kind of affiliations with or involvement in any organization or entity with any financial interest (such as honoraria; educational grants; participation in speakers' bureaus; membership, employment, consultancies, stock ownership, or other equity interest; and expert testimony or patent-licensing arrangements), or non-financial interest (such as personal or professional relationships, affiliations, knowledge or beliefs) in the subject matter or materials discussed in this manuscript

References

1. Flaig, T. W. *et al.* Bladder Cancer, Version 3.2020, NCCN Clinical Practice Guidelines in Oncology. *J Natl Compr Canc Netw* **18**, 329-354, doi:10.6004/jnccn.2020.0011 (2020).
2. Chang, S. S. *et al.* Diagnosis and Treatment of Non-Muscle Invasive Bladder Cancer: AUA/SUO Guideline. *J Urol* **196**, 1021-1029, doi:10.1016/j.juro.2016.06.049 (2016).
3. Chavan, S., Bray, F., Lortet-Tieulent, J., Goodman, M. & Jemal, A. International variations in bladder cancer incidence and mortality. *Eur Urol* **66**, 59-73, doi:10.1016/j.eururo.2013.10.001 (2014).
4. Sylvester, R. J. *et al.* Predicting recurrence and progression in individual patients with stage Ta T1 bladder cancer using EORTC risk tables: a combined analysis of 2596 patients from seven EORTC trials. *Eur Urol* **49**, 466-465; discussion 475-467, doi:10.1016/j.eururo.2005.12.031 (2006).
5. Mookerjee, S. A. & Brand, M. D. Measurement and Analysis of Extracellular Acid Production to Determine Glycolytic Rate. *J Vis Exp*, e53464, doi:10.3791/53464 (2015).
6. Sylvester, R. J. *et al.* Systematic Review and Individual Patient Data Meta-analysis of Randomized Trials Comparing a Single Immediate Instillation of Chemotherapy After Transurethral Resection with Transurethral Resection Alone in Patients with Stage pTa-pT1 Urothelial Carcinoma of the Bladder: Which Patients Benefit from the Instillation? *Eur Urol* **69**, 231-244, doi:10.1016/j.eururo.2015.05.050 (2016).
7. Pan, J., Liu, M. & Zhou, X. Can intravesical bacillus Calmette-Guerin reduce recurrence in patients with non-muscle invasive bladder cancer? An update and cumulative meta-analysis. *Front Med* **8**, 241-249, doi:10.1007/s11684-014-0328-0 (2014).
8. Veeratterapillay, R., Heer, R., Johnson, M. I., Persad, R. & Bach, C. High-Risk Non-Muscle-Invasive Bladder Cancer-Therapy Options During Intravesical BCG Shortage. *Curr Urol Rep* **17**, 68,

doi:10.1007/s11934-016-0625-z (2016).

9. Sylvester, R. J., van der Meijden, A. P., Witjes, J. A. & Kurth, K. Bacillus calmette-guerin versus chemotherapy for the intravesical treatment of patients with carcinoma in situ of the bladder: a meta-analysis of the published results of randomized clinical trials. *J Urol* **174**, 86-91; discussion 91-82, doi:10.1097/01.ju.0000162059.64886.1c (2005).
10. Lamm, D. L., Stogdill, V. D., Stogdill, B. J. & Crispen, R. G. Complications of bacillus Calmette-Guerin immunotherapy in 1,278 patients with bladder cancer. *J Urol* **135**, 272-274, doi:10.1016/s0022-5347(17)45606-0 (1986).
11. Gontero, P. *et al.* The impact of intravesical gemcitabine and 1/3 dose Bacillus Calmette-Guerin instillation therapy on the quality of life in patients with nonmuscle invasive bladder cancer: results of a prospective, randomized, phase II trial. *J Urol* **190**, 857-862, doi:10.1016/j.juro.2013.03.097 (2013).
12. Lu, J. L. *et al.* Efficacy of intravesical therapies on the prevention of recurrence and progression of non-muscle-invasive bladder cancer: A systematic review and network meta-analysis. *Cancer Med-Us* **9**, 7800-7809, doi:10.1002/cam4.3513 (2020).
13. Honigsmann, H. Phototherapy and photochemotherapy. *Semin Dermatol* **9**, 84-90 (1990).
14. Matz, H. Phototherapy for psoriasis: what to choose and how to use: facts and controversies. *Clin Dermatol* **28**, 73-80, doi:10.1016/j.clindermatol.2009.04.003 (2010).
15. Teixeira, A. F., Alves, J. R., de Souza da Fonseca, A. & Mencalha, A. L. Low power blue LED exposure increases effects of doxorubicin on MDA-MB-231 breast cancer cells. *Photodiagnosis Photodyn Ther* **24**, 250-255, doi:10.1016/j.pdpdt.2018.07.016 (2018).
16. Lin, Y. C. *et al.* Acridine orange exhibits photodamage in human bladder cancer cells under blue light exposure. *Sci Rep* **7**, 14103, doi:10.1038/s41598-017-13904-0 (2017).
17. Oplander, C. *et al.* Mechanism and biological relevance of blue-light (420-453 nm)-induced nonenzymatic nitric oxide generation from photolabile nitric oxide derivates in human skin in vitro and in vivo. *Free Radic Biol Med* **65**, 1363-1377, doi:10.1016/j.freeradbiomed.2013.09.022 (2013).
18. Oplander, C. *et al.* Effects of blue light irradiation on human dermal fibroblasts. *J Photochem Photobiol B* **103**, 118-125, doi:10.1016/j.jphotobiol.2011.02.018 (2011).
19. Taflinski, L. *et al.* Blue light inhibits transforming growth factor-beta1-induced myofibroblast differentiation of human dermal fibroblasts. *Exp Dermatol* **23**, 240-246, doi:10.1111/exd.12353 (2014).
20. Yan, G. *et al.* Blue light emitting diodes irradiation causes cell death in colorectal cancer by inducing ROS production and DNA damage. *Int J Biochem Cell Biol* **103**, 81-88, doi:10.1016/j.biocel.2018.08.006 (2018).
21. Zhuang, J. *et al.* Blue light-induced apoptosis of human promyelocytic leukemia cells via the mitochondrial-mediated signaling pathway. *Oncol Lett* **15**, 6291-6296, doi:10.3892/ol.2018.8162 (2018).

22. Ohara, M., Kawashima, Y., Katoh, O. & Watanabe, H. Blue light inhibits the growth of B16 melanoma cells. *Jpn J Cancer Res* **93**, 551-558, doi:10.1111/j.1349-7006.2002.tb01290.x (2002).
23. Lewis, J. B. *et al.* Blue light differentially alters cellular redox properties. *J Biomed Mater Res B Appl Biomater* **72**, 223-229, doi:10.1002/jbm.b.30126 (2005).
24. Omata, Y. *et al.* Intra- and extracellular reactive oxygen species generated by blue light. *J Biomed Mater Res A* **77**, 470-477, doi:10.1002/jbm.a.30663 (2006).
25. Sato, K., Minai, Y. & Watanabe, H. Effect of monochromatic visible light on intracellular superoxide anion production and mitochondrial membrane potential of B16F1 and B16F10 murine melanoma cells. *Cell Biol Int* **37**, 633-637, doi:10.1002/cbin.10069 (2013).
26. Garza, Z. C. F., Born, M., Hilbers, P. A. J., van Riel, N. A. W. & Liebmann, J. Visible Blue Light Therapy: Molecular Mechanisms and Therapeutic Opportunities. *Curr Med Chem* **25**, 5564-5577, doi:10.2174/0929867324666170727112206 (2018).
27. Hohn, A. *et al.* Distinct mechanisms contribute to acquired cisplatin resistance of urothelial carcinoma cells. *Oncotarget* **7**, 41320-41335, doi:10.18632/oncotarget.9321 (2016).
28. Cummings, J., Spanswick, V. J. & Smyth, J. F. Re-evaluation of the molecular pharmacology of mitomycin C. *Eur J Cancer* **31A**, 1928-1933, doi:10.1016/0959-8049(95)00364-9 (1995).
29. Song, X. *et al.* Hypoxia Promotes Synergy between Mitomycin C and Bortezomib through a Coordinated Process of Bcl-xL Phosphorylation and Mitochondrial Translocation of p53. *Mol Cancer Res* **13**, 1533-1543, doi:10.1158/1541-7786.MCR-15-0237 (2015).
30. Chen, S. K. *et al.* Hydrostatic pressure enhances mitomycin C induced apoptosis in urothelial carcinoma cells. *Urol Oncol* **32**, 26 e17-24, doi:10.1016/j.urolonc.2012.09.004 (2014).
31. Speers, A. G., Lwaleed, B. A., Featherstone, J. M. & Cooper, A. J. Multidrug resistance in a urothelial cancer cell line after 3, 1-hour exposures to mitomycin C. *J Urol* **178**, 2171-2175, doi:10.1016/j.juro.2007.06.047 (2007).
32. Riccardi, C. & Nicoletti, I. Analysis of apoptosis by propidium iodide staining and flow cytometry. *Nature protocols* **1**, 1458-1461, doi:10.1038/nprot.2006.238 (2006).
33. Pandurangan, M. *et al.* beta-Alanine intercede metabolic recovery for amelioration of human cervical and renal tumors. *Amino Acids* **49**, 1373-1380, doi:10.1007/s00726-017-2437-y (2017).
34. Albers, I. *et al.* Blue light (lambda=453nm) nitric oxide dependently induces beta-endorphin production of human skin keratinocytes in-vitro and increases systemic beta-endorphin levels in humans in-vivo. *Free Radic Biol Med* **145**, 78-86, doi:10.1016/j.freeradbiomed.2019.09.022 (2019).
35. Chavan, H. *et al.* Arsenite Effects on Mitochondrial Bioenergetics in Human and Mouse Primary Hepatocytes Follow a Nonlinear Dose Response. *Oxid Med Cell Longev* **2017**, 9251303, doi:10.1155/2017/9251303 (2017).
36. Butler, M. G., Hossain, W. A., Tessman, R. & Krishnamurthy, P. C. Preliminary observations of mitochondrial dysfunction in Prader-Willi syndrome. *Am J Med Genet A* **176**, 2587-2594, doi:10.1002/ajmg.a.40526 (2018).

37. Brodsky, M., Abrouk, M., Lee, P. & Kelly, K. M. Revisiting the History and Importance of Phototherapy in Dermatology. *JAMA Dermatol* **153**, 435, doi:10.1001/jamadermatol.2017.0722 (2017).
38. Honigsmann, H. History of phototherapy in dermatology. *Photochem Photobiol Sci* **12**, 16-21, doi:10.1039/c2pp25120e (2013).
39. Pillai, S., Oresajo, C. & Hayward, J. Ultraviolet radiation and skin aging: roles of reactive oxygen species, inflammation and protease activation, and strategies for prevention of inflammation-induced matrix degradation - a review. *Int J Cosmet Sci* **27**, 17-34, doi:10.1111/j.1467-2494.2004.00241.x (2005).
40. Yang, M. Y., Chang, C. J. & Chen, L. Y. Blue light induced reactive oxygen species from flavin mononucleotide and flavin adenine dinucleotide on lethality of HeLa cells. *J Photochem Photobiol B* **173**, 325-332, doi:10.1016/j.jphotobiol.2017.06.014 (2017).
41. Liang, J. Y., Cheng, C. W., Yu, C. H. & Chen, L. Y. Investigations of blue light-induced reactive oxygen species from flavin mononucleotide on inactivation of E. coli. *J Photochem Photobiol B* **143**, 82-88, doi:10.1016/j.jphotobiol.2015.01.005 (2015).
42. Nakanishi-Ueda, T. *et al.* Blue LED light exposure develops intracellular reactive oxygen species, lipid peroxidation, and subsequent cellular injuries in cultured bovine retinal pigment epithelial cells. *Free Radic Res* **47**, 774-780, doi:10.3109/10715762.2013.829570 (2013).
43. Guan, R. *et al.* A review of dietary phytochemicals and their relation to oxidative stress and human diseases. *Chemosphere* **271**, 129499, doi:10.1016/j.chemosphere.2020.129499 (2021).
44. Poprac, P. *et al.* Targeting Free Radicals in Oxidative Stress-Related Human Diseases. *Trends Pharmacol Sci* **38**, 592-607, doi:10.1016/j.tips.2017.04.005 (2017).
45. Koppula, S., Kumar, H., Kim, I. S. & Choi, D. K. Reactive oxygen species and inhibitors of inflammatory enzymes, NADPH oxidase, and iNOS in experimental models of Parkinson's disease. *Mediators Inflamm* **2012**, 823902, doi:10.1155/2012/823902 (2012).
46. Arthaut, L. D. *et al.* Blue-light induced accumulation of reactive oxygen species is a consequence of the Drosophila cryptochrome photocycle. *PloS one* **12**, e0171836, doi:10.1371/journal.pone.0171836 (2017).
47. Hockberger, P. E. *et al.* Activation of flavin-containing oxidases underlies light-induced production of H2O2 in mammalian cells. *Proc Natl Acad Sci U S A* **96**, 6255-6260, doi:10.1073/pnas.96.11.6255 (1999).
48. Krassovka, J. M. *et al.* The impact of non-toxic blue light (453 nm) on cellular antioxidative capacity, TGF-beta1 signaling, and myofibrogenesis of human skin fibroblasts. *J Photochem Photobiol B* **209**, 111952, doi:10.1016/j.jphotobiol.2020.111952 (2020).
49. Liebmann, J., Born, M. & Kolb-Bachofen, V. Blue-light irradiation regulates proliferation and differentiation in human skin cells. *J Invest Dermatol* **130**, 259-269, doi:10.1038/jid.2009.194 (2010).
50. Su, L. J. *et al.* Reactive Oxygen Species-Induced Lipid Peroxidation in Apoptosis, Autophagy, and Ferroptosis. *Oxid Med Cell Longev* **2019**, 5080843, doi:10.1155/2019/5080843 (2019).

51. Circu, M. L. & Aw, T. Y. Reactive oxygen species, cellular redox systems, and apoptosis. *Free Radic Biol Med* **48**, 749-762, doi:10.1016/j.freeradbiomed.2009.12.022 (2010).
52. Nicotera, P. & Melino, G. Regulation of the apoptosis-necrosis switch. *Oncogene* **23**, 2757-2765, doi:10.1038/sj.onc.1207559 (2004).

Figures

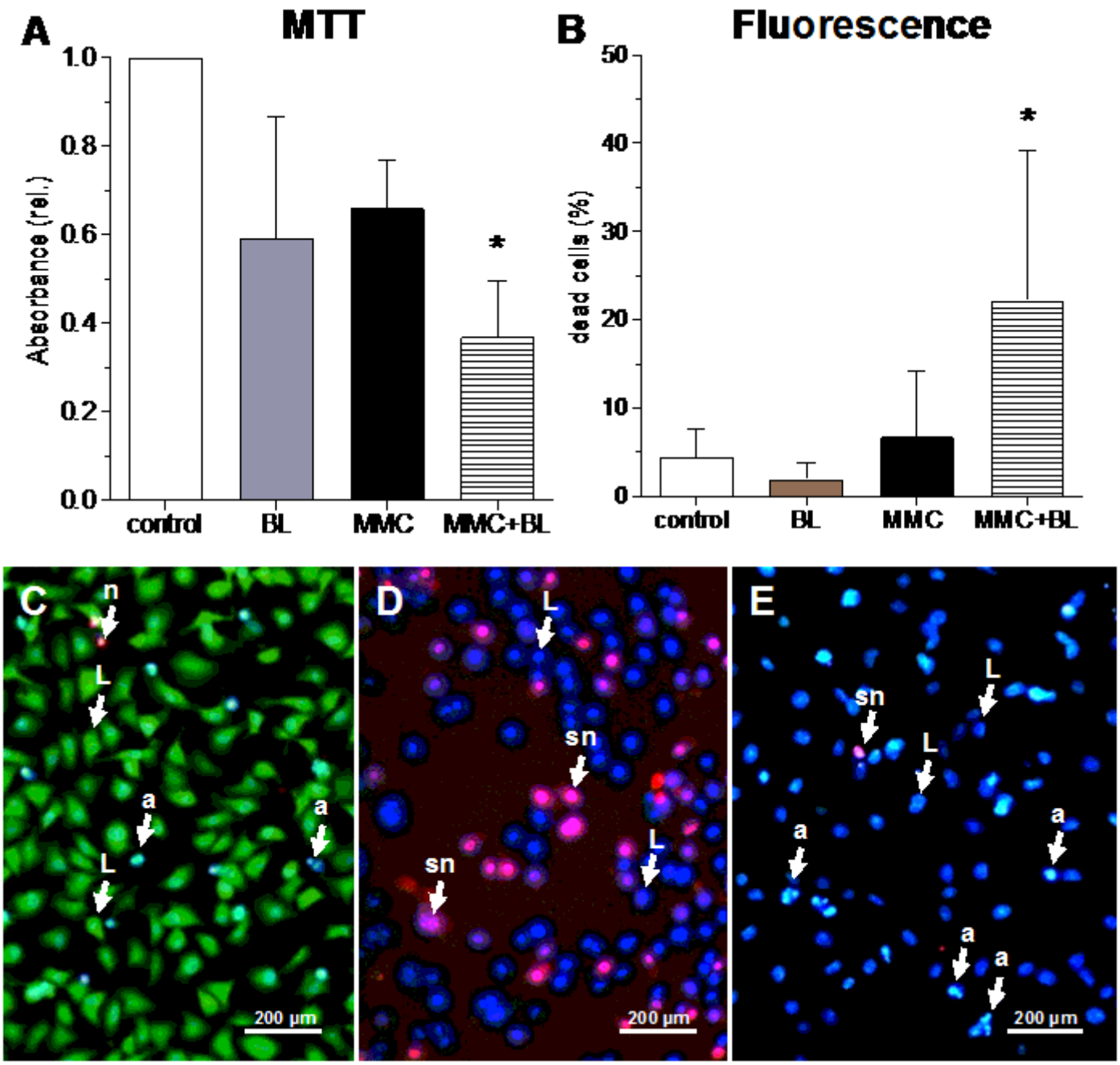

Figure 1

Impact of blue light (453 nm) and Mitomycin C on cell death of RT112 cells. Bars shown in **A** and **B** represent mean ± SD of eight (**A**) or six (**B**) individual experiments. Shown are values of the non-treated

control cultures (100%, white bar), blue light irradiated cultures (**BL**, 110 J/cm^2, grey bar), Mitomycin C treated cultures (**MMC**, 10 µg/ml, black bar), and **MMC+BL** treated cultures (striped bar). *, $p<0.05$ as compared to the values of the other three bars. **A,** relative number of living cells, detected by the MTT assay, in RT112 cell cultures treated as indicated. **B**, relative number of dead cells in RT112 cell cultures treated as indicated by using different fluorochromes for the detection of living cells (fluorescein diacetate - FDA, 2 µg/ml), necrotic cells (propidium iodide - PI, 0.5 µg/ml) and visualization of the nuclear morphology of living or apoptotic cell nuclei (H33342 dye, 0.5 µg/ml). **C, D, E**: By choosing the appropriate fluorescence filter, it was possible to differentiate between the different vitality states of the cells. **C**, living cells (**L**, green colored by FDA), necrotic nuclei (**n**, red colored by PI), pyknotic and/or fragmented apoptotic nuclei (**a**, blue colored by H33342). **D**, Intact cell nuclei of living cells (**L**, blue colored by H33342), secondary necrosis (**sn**, red colored by PI). **E**, secondary necrosis (**sn**, red colored by PI), pyknotic and/or fragmented apoptotic nuclei (**a**, blue colored by H33342).

03 Pia ·
Dissertia

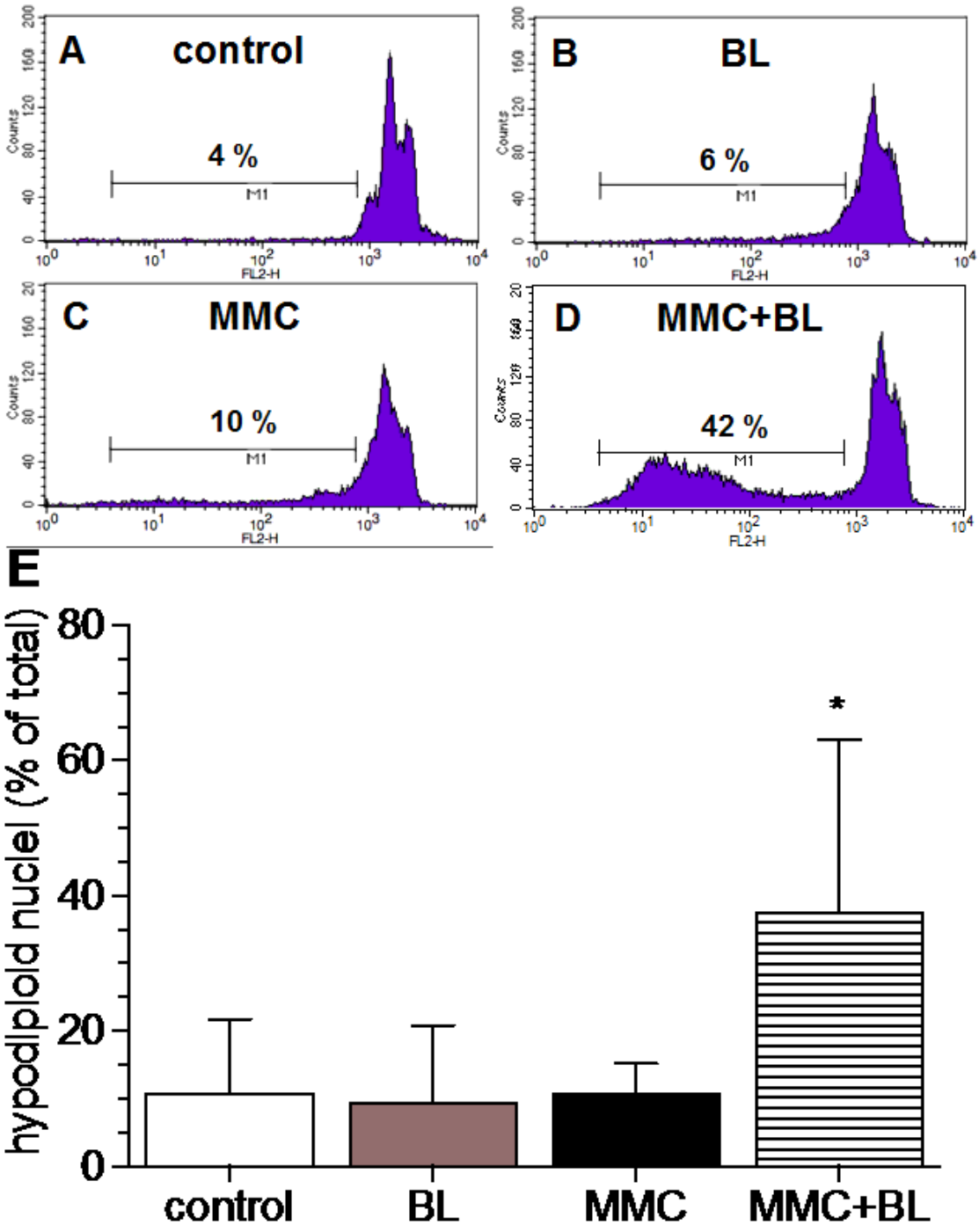

Figure 2

Impact of blue light (453 nm) and Mitomycin C on apoptotic cell death of RT112 cells. With the help of FACS technology, we have detected the relative proportion of apoptotic cells with hypodiploid cell nuclei according to Riccardi and Nicoletti [32] in both untreated and treated RT112 tumor cell cultures. **A-D**, FACS-histograms of an individual representative experiment. **A**, non-treated **control** cultures**; B**, blue light irradiated cultures (**BL**, 110 J/cm^2); **C**, Mitomycin C treated cultures (**MMC**, 10 µg/ml); **D**, blue light

irradiation of Mitomycin C treated cultures (**MMC+BL)**. **D**, Quantitative evaluation of apoptotic cells with hypodiploid cell nuclei of the control cultures (**control**, white bar), blue light irradiated cultures (**BL**, 110 J/cm^2, grey bar), Mitomycin C treated cultures (**MMC**, 10 µg/ml, black bar), and blue light exposed Mitomycin C treated cultures (**MMC+BL**, striped bar). Bars represent the mean ± SD of four individual experiments. *, p<0.05 as compared to the values of the other three bars.

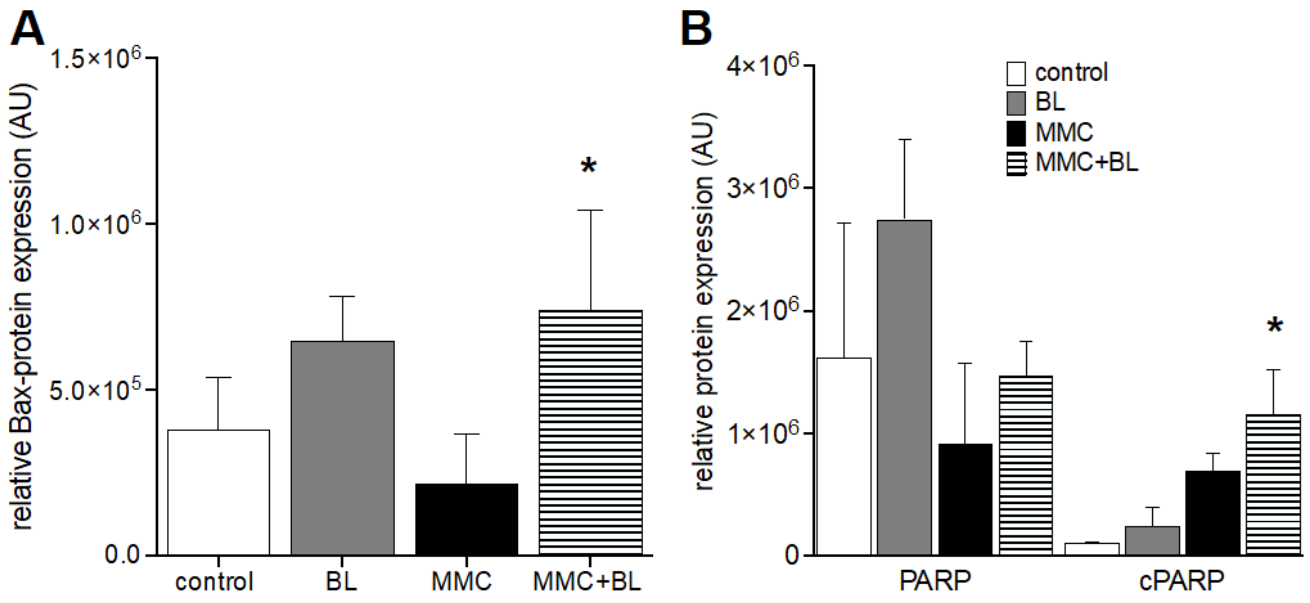

Figure 3

Impact of blue light (453 nm) and Mitomycin C induced cell death of RT112 cells. Bars shown in **A** and **B** represent mean ± SD of six individual experiments. Shown are values of the non-treated control cultures (100%, white bars), blue light irradiated cultures (**BL**, 110 J/cm^2, grey bars), Mitomycin C treated cultures (**MMC**, 10 µg/ml, black bar), and blue light exposed Mitomycin C treated cultures (**MMC+BL,** striped bars). **A,** Bax protein expression. *, p<0.05 as compared to the values RT112 tumor cell cultures treated only with Mitomycin C (**MMC**, black bar). **B**, PARP protein expression and caspase-3 dependent PARP-cleavage (**cPARP**).

*, p<0.05 as compared to the cPARP values represented by the other three bars.

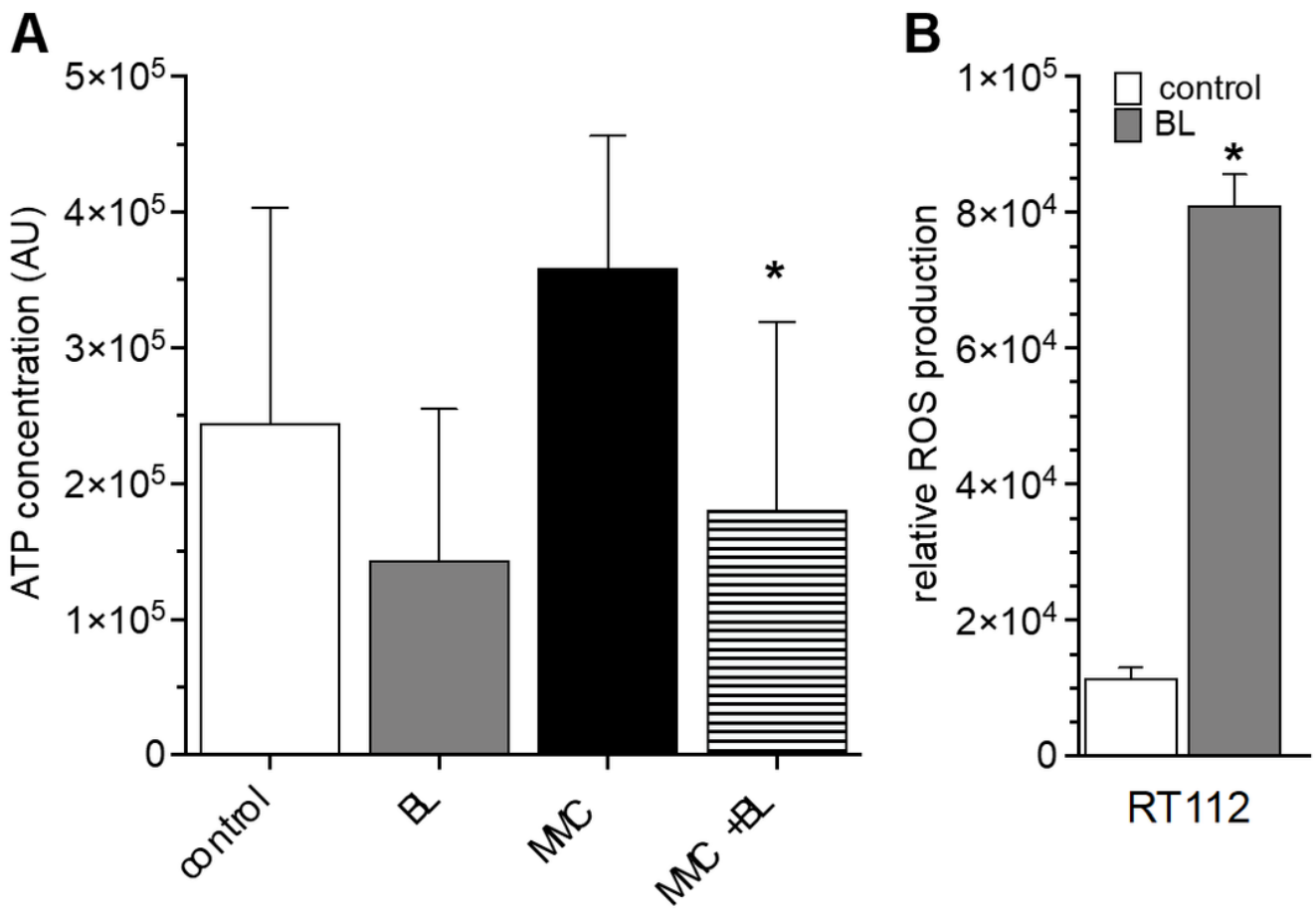

Figure 4

Impact of blue light (453 nm) and Mitomycin C induced on ATP production and intracellular ROS formation of RT112 cells. Bars shown in **A** represent mean ± SD of six individual experiments. Shown are values of the non-treated control cultures (100%, white bar), blue light irradiated cultures (**BL**, 110 J/cm^2, grey bar), Mitomycin C treated cultures (**MMC**, 10 µg/ml, black bar), and blue light exposed Mitomycin C treated cultures (**MMC+BL,** striped bar). **A,** ATP concentration in RT112 tumor cell cultures. *, $p<0.05$ as compared to the values RT112 tumor cell cultures treated only with Mitomycin C (**MMC**, black bar). **B**, Intracellular ROS generation in non-treated (**control**, white bar) and blue light irradiated (**BL**, grey bar, 110 J/cm^2) RT112 tumor cell cultures. *, $p<0.05$

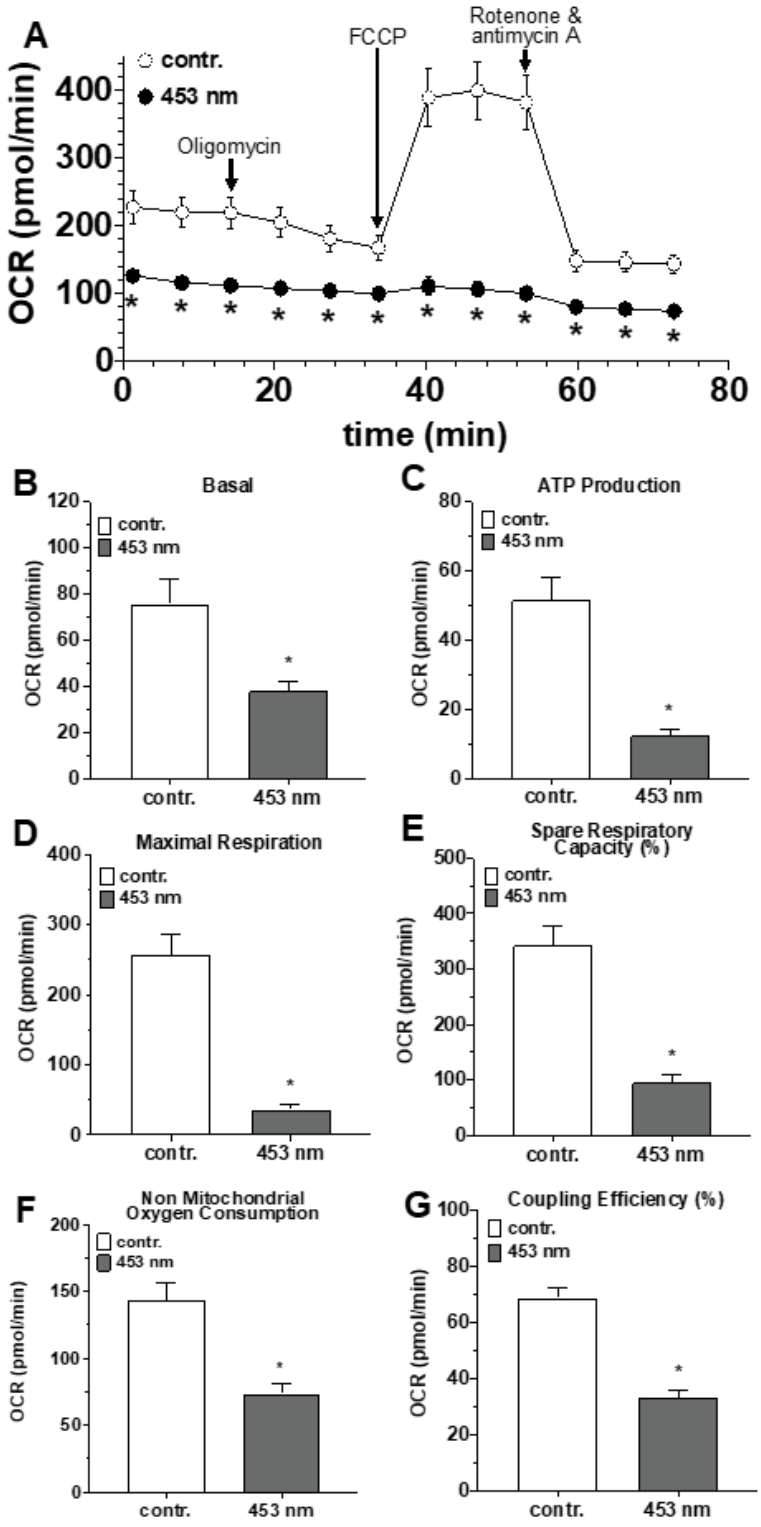

Figure 5

Modulation of mitochondrial respiration of RT112 tumor cells by blue light. Oxygen consumption rate (**OCR** in pmol/min) of 3x10^4 RT112 tumor cells/well was measured under basal conditions (**A**, open circles; **B-G**, white bars) or one hour after irradiation with blue light (110 J/cm^2, **A**, black circles; **B-G**, grey bars) followed by the sequential addition of oligomycin (0.25 µM), FCCP (1 µM), and rotenone plus antimycin A (1 µM), as indicated. Each data point represents the mean ± SD of 12 individual OCR values.

*, $p<0.05$ as compared to the corresponding values obtained under basal conditions. **B-G**, the assay reports multiple key parameters, including basal respiration (**B**), ATP-linked respiration (**C**), maximal respiration (**D**), spare respiratory capacity (**E**), non-mitochondrial oxygen consumption (**F**), and coupling efficiency (**G**). Bars represent the mean ± SD of 12 individual OCR values obtained under basal conditions (white bars) or one hour after light exposure (grey bars). $p<0.05$ as compared to the corresponding values obtained under basal conditions.

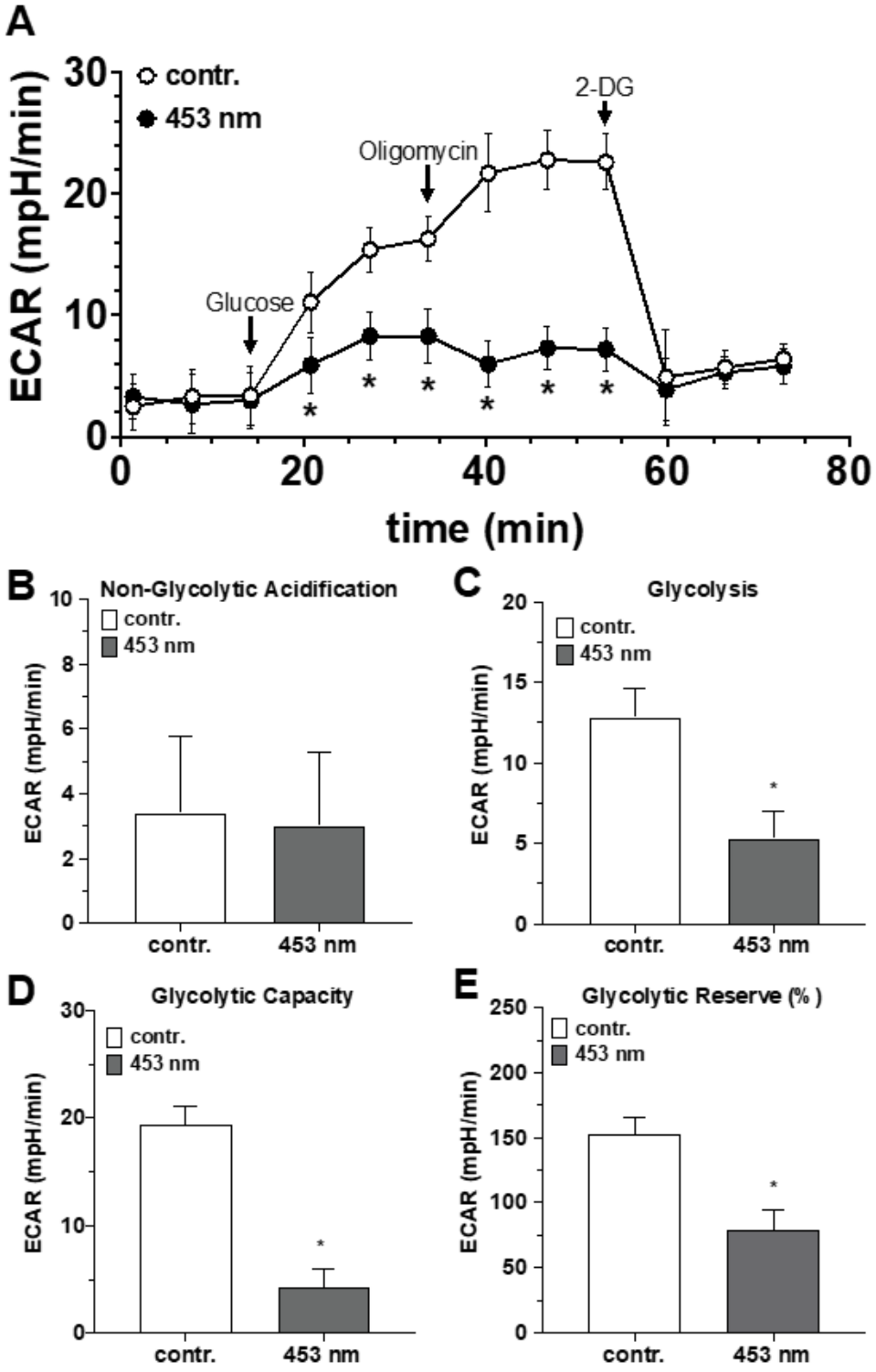

Figure 6

Modulation of glycolysis of RT112 tumor cells by blue light. A, kinetic of extracellular acidification responses (**ECAR** in mpH/min) of $3x10^4$ RT112 tumor cells/well to glucose (10 mM), oligomycin (0.25 µM), and 2-Desoxy-D-glucose (2-DG, 100 mM) was measured under basal conditions (open circles) or one hour after irradiation with blue light (110 J/cm^2, black circles. Each data point represents the mean ± SD of 12 individual ECAR values. *, $p<0.05$ as compared to the corresponding values obtained under basal

conditions. **B-E**, the assay reports multiple key parameters, including non-glycolytic acidification (**B**), glycolysis (**C**), glycolytic capacity (**D**), and glycolytic reserve (**E**). Bars represent the mean ± SD of 12 individual ECAR values obtained under basal conditions (white bars) or one hour after light exposure (grey bars). $p<0.05$ as compared to the corresponding values obtained under basal conditions.